J. Inst. Eng. India Ser. C (December 2021) 102(6):1553–1563
https://doi.org/10.1007/s40032-021-00753-0

ORIGINAL CONTRIBUTION

Temperature Field Analysis of Engine's Energy Recovery System using Fluid–Structure Coupling

Ping Xu[1]

Received: 8 March 2021 / Accepted: 27 August 2021 / Published online: 16 September 2021

Abstract At present, internal combustion engines (ICE) are still the main power source for cars, and about 60% of the fuel energy is wasted through exhaust gas and cooling system of ICE. One of the methods for energy recovery of ICE is to use thermoelectric generator (TEG). To improve the energy recovery efficiency of TEG, the temperature distribution over the cooling system should be known. For this purpose, the temperature filed of a TEG is analyzed using ANSYS software. In this paper, some inner structures of TEG are designed and their temperature fields are simulated. Through comparing the simulation with experimental results, the design with inclined symmetrical baffles can generate the most uniform temperature distribution. Then, this design is used to further simulate the cooling capacity of the TEG. The results show that the impact of thermal radiation should be considered in the TEG simulation; otherwise large errors will be generated. It also can be seen that the cooling method using solid plate connecting with a solid column has limitation because most of the heat is concentrated in the solid plate, and it should be optimized in further research.

Keywords Internal combustion engine · Thermoelectric generation · Temperature · Cooling capacity

✉ Ping Xu
thinkjump01@163.com

[1] Department of Civil Engineering, Henan Institute of Engineering, Zhengzhou, China

Introduction

More and more cars are going into families in recent years, and new automotive technologies, such as alternative fuel, electrification and hybrid, have been adopted. At present, although ICE is still the most important power source for vehicles, the thermal efficiency of ICE is not high enough. Therefore, many technologies have been put forward to improve Ice's the thermal efficiency [1–3].

TEG is a new kind of energy recovery technology which can convert heat into electricity directly using the Seebeck effect of thermoelectric materials [4, 5], which has been recognized to have many advantages, such as stable performance, free of noise and wear, small size, light weight, long life and so on. More and more attention have been paid to TEG in recent years [6]. The effects of thermoelectric structure [7], cooling method [8–10], heat sink length [11] and radiator structure [12] on the heat transfer efficiency of TEG have been studied. However, only a few of researches focused on coolant energy recovery, and only one application using TEG to replace the radiator was reported, which showed that at the speed of 80 km/h the TEG's energy recovery efficiency was 3.2% while at idle speed the energy recovery efficiency increased up to 10% [13]. The main cause for the lack of researches on coolant energy recovery is the low temperature in cooling system which is generally lower than 110 °C and is much lower than the exhaust gas temperature. However, in the view of engine heat balance, the coolant waste energy is also considerable large compared to the engine exhaust gas energy [13]. Considering that the cooling system has cooling fans and pumps, which can provide good premise for TEG cooling, and the allowable temperature of commercially available TEG modules is 220 °C, which is higher than the coolant temperature, so commercial TEG

modules can be very conveniently used for coolant energy recovery.

Researches have shown that TEG module's thermal resistance increases with temperature rise, which means the characteristics of TEG can be affected by temperature, and the maximum power can increase with the temperature difference [14]. It also indicates that replacing the radiator with TEG radiator for recovering energy is feasible, and energy recovery efficiency of TEG can reach 10% at idle condition [15, 16].

In order to recover energy from the cooling system, one TEG has been developed in our previous study [9], but there is no universally applicable method for the design of energy recovery structure. Therefore, the structure design of TEG is studied by simulation in this paper, including the inner pipe structure and cooling capacity.

Structure of the Engine Energy Recovery System Based on TEG

There is no standard structure for the TEG-based ICE energy recovery system, and the common structure of the energy recovery system is shown in Fig. 1 which consists of six parts. The first part is energy recovery pipe which is coupled with the engine cooling system and is also the hot end of the TEG. The second part is the TEG modules which are the main part of the TEG system and can convert heat into electricity directly. The third part is the connection structure which is used to connect the TEG system. The fourth part is the radiator which is made up of fins and is used to radiate the heat. The fifth part is the solid columns used to connect the radiator and solid plate. The sixth part is the solid plate which is in contact with the cold end of the TEG.

The dimension of the energy recovery system is based on the original radiator and the height of the solid plate is half of the original radiator while the width is kept the same. In order to ensure the cooling capacity, the longitudinal dimension of upper portion is increased with heat sink, and the longitudinal dimension is also half of the original heat sink. Therefore, the longitudinal dimension of energy recovery system remains the same as the original radiator.

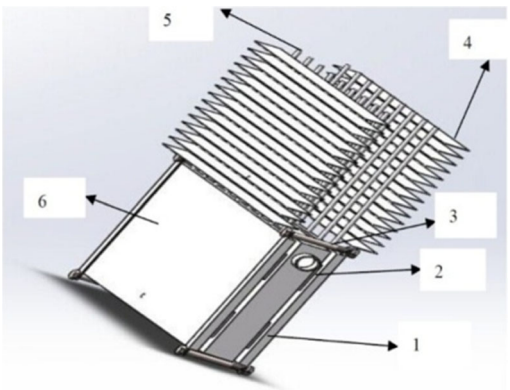

1-pipe; 2-TEG chips; 3-connection; 4-radiator; 5-solid columns; 6-solid plate

Fig. 1 Structure of engine recovery system

Analysis of Internal Structure of the Pipe

More homogeneous temperature distribution on the surface of energy recovery pipe can improve the output power of TEG, so the pipe was designed as a rectangular box structure with inner separators. Several designs on separator arrangement were proposed, as shown in Fig. 2.The width is 300 mm and length is 1000 mm and the solid model is established using solid works software.

Briefly, Type (a) consists of parallel separators; Type (b) consists of symmetrical separators with the angles of 60 degree, 45 degree and 30 degree to the central axis, respectively; Type (c) consists of two V-shaped separators; Type (d) consists of the similar structure to Type (b) but with a baffle at the entrance. Temperature fields were then analyzed for those different type structures.

Modeling

The modeling process was identical for the four different types of pipe design, and Type (a) is selected as an example to describe this process.

Solid Models

Because the analysis needs to couple fluid and solid phases, the solid phase model and the fluid phase model should be established separately. The fluid phase model was the inner of the pipe while the solid phase model was the shell. The models for Type (a) are presented in Fig. 3, in which Fig. 3a is the solid phase of the pipe, Fig. 3b is the fluid phase, and Fig. 3c is the compound of solid and liquid phases.

Meshing

The coolant flow was analyzed using Fluent, of which the interface is shown in Fig. 4.Then, the meshing process was done in meshing interface. The maximum mesh size was 0.0001 m and mesh level was medium, meanwhile the inlet, outlet and symmetry were defined separately. Then, the whole fluid mesh is illustrated in Fig. 5.

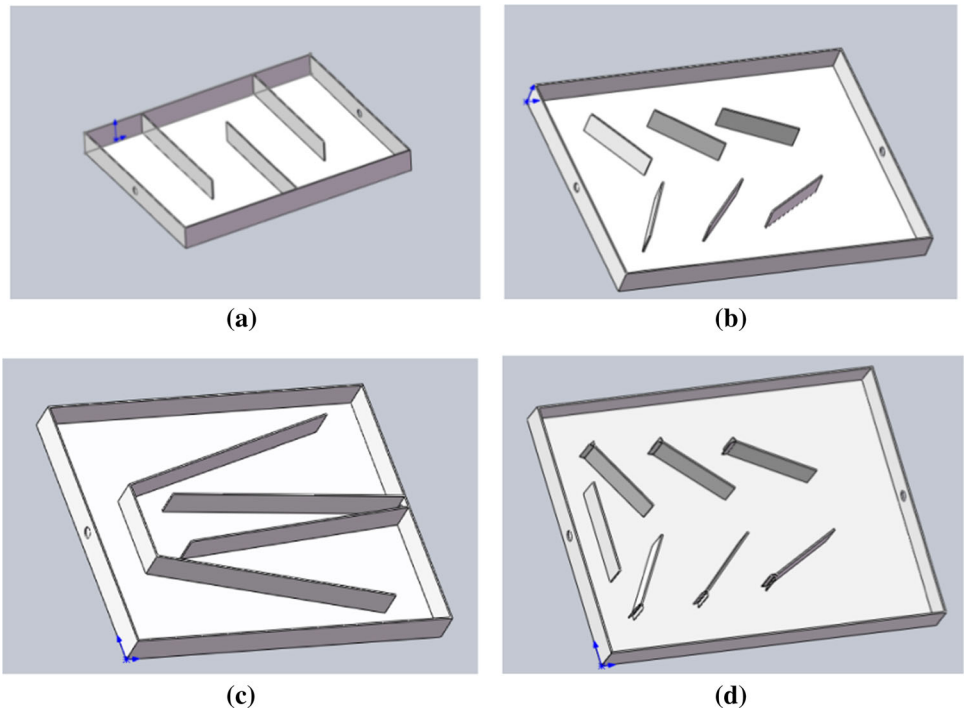

Fig. 2 Internal structures of pipe for TEG

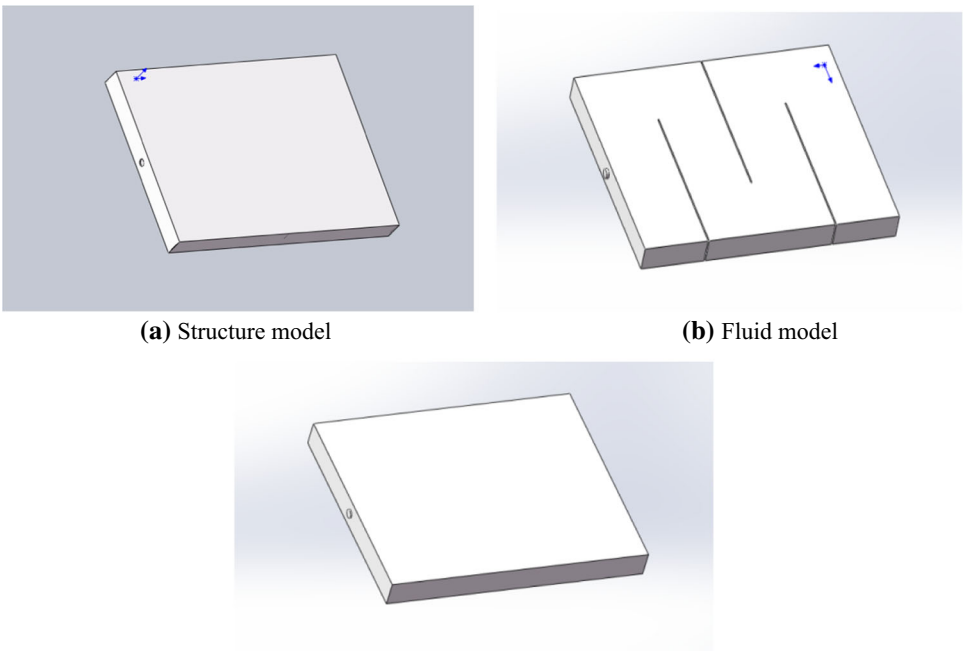

Fig. 3 Models of type **a**

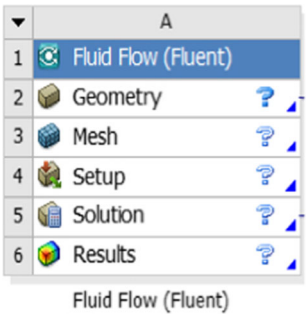

Fig. 4 Activated fluent

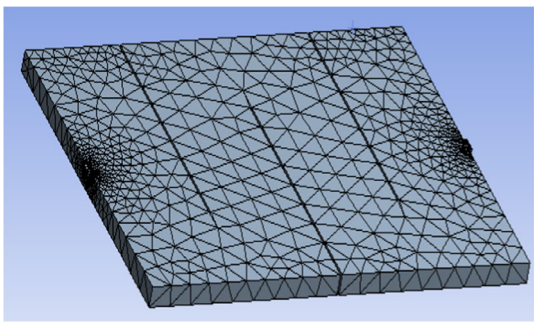

Fig. 5 Mesh model of fluid

Governing Equations

The governing equations include mass conservation equation, momentum equation, and energy equation which are shown in following.

$$\frac{\partial u_x}{\partial x}+\frac{\partial u_y}{\partial y}+\frac{\partial u_z}{\partial z}=0 \tag{1}$$

where u_x-x axis velocity; u_y-y axis velocity; u_z-z axis velocity.

X axis momentum equation

$$\frac{Du_x}{Dt}=\rho g_x-\frac{1}{\rho}\frac{\partial p}{\partial x}+\frac{\partial}{\partial x}\left[\mu\left(\frac{\partial u_x}{\partial y}+\frac{\partial u_y}{\partial x}-\frac{2}{3}\frac{\partial u_z}{\partial z}\delta_{xy}\right)\right] \tag{2}$$

Y axis momentum equation

$$\frac{Du_y}{Dt}=\rho g_y-\frac{1}{\rho}\frac{\partial p}{\partial y}+\frac{\partial}{\partial y}\left[\mu\left(\frac{\partial u_x}{\partial y}+\frac{\partial u_y}{\partial x}-\frac{2}{3}\frac{\partial u_z}{\partial z}\delta_{yz}\right)\right] \tag{3}$$

Z axis momentum equation

$$\frac{Du_z}{Dt}=\rho g_z-\frac{1}{\rho}\frac{\partial p}{\partial z}+\frac{\partial}{\partial z}\left[\mu\left(\frac{\partial u_x}{\partial y}+\frac{\partial u_y}{\partial x}-\frac{2}{3}\frac{\partial u_z}{\partial z}\delta_{zx}\right)\right] \tag{4}$$

where p-the static pressure; μ-Molecular viscosity coefficient.

Energy equation

$$\rho\frac{DH}{Dt}=\rho q_g++\frac{\partial}{\partial x_i}\left(\tau_{ij}U_j\right)+\frac{\partial}{\partial x_j}\left(\lambda\frac{\partial T}{\partial x_j}\right) \tag{5}$$

where H-total enthalpy; T-temperature;τ_{ij}-deviator stress tensor;q_g-heat flux; i, j-x, y, z.

Boundary Conditions

Steady-state calculation was selected. The density of the coolant (mixture of water and antifreeze) was 1010 kg/m^3, while the kinematic viscosity was 0.0011 Pa·s for the k-ε turbulence model.

It should be noted that in actual engine the coolant temperature usually varies from 85 to 95 °C. Therefore, the coolant temperature in simulation is set as 85 °C with an inlet velocity of 0.5 m/s. The outlet pressure is 101000 Pa and is defined as a pressure boundary condition.

Since the material of pipe is aluminum, it is necessary to build an aluminum alloy material parameters data base in the software. This work can be made by adding aluminum material in engineering data modifying interface. The modification is shown in Fig. 6, in which the density is set as 2700 kg/m^3, Young's modulus 72e + 7Paand Poisson's ratio 0.33.

Coupling between fluid and solid calculation was completed by adding a solid module into the ANSYS workbench interface. Then, the data could be transmitted between the different modules, so the results from fluid phase calculation could be set as the boundary conditions of solid phase analysis, so the inner surface of the pipe is selected as an interface where the results from fluid phase calculation are transmitted to the solid phase analysis. And both ends of the pipe were fixed with solid constraints for the solid phase simulation. The coupled modules are shown in Fig. 7.

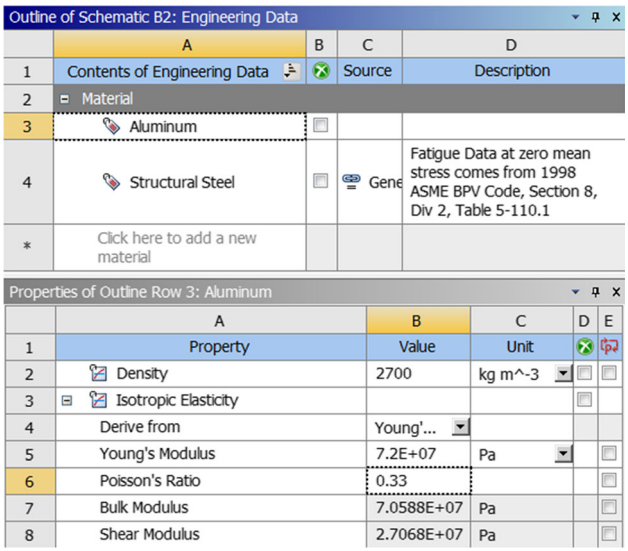

Fig. 6 Material property modification

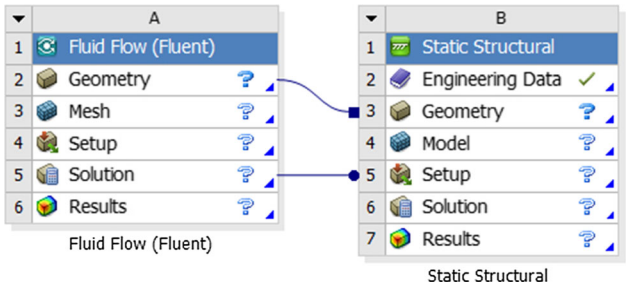

Fig. 7 Coupled models of fluid and structure

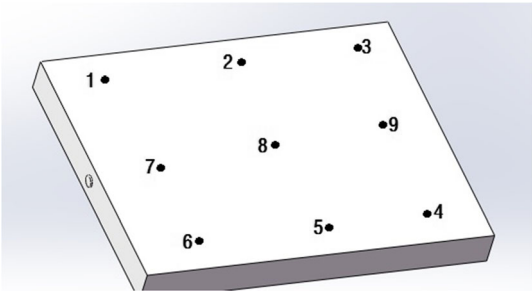

Fig. 8 Measured points view

Table 1 Parameters of the t thermocouple

Parameters(unit)	Range	Resolution	Error
Temperature(°C)	0 ~ 800	0.1	± 0.5

Model Validation

In order to validate the model, the temperature of the surface is measured according to the simulation sets.

The temperature of 9 measured points are measured which are shown in Fig. 8. And the temperature is measured by K type thermocouple and the parameters of thermocouple are listed in Table1.Meanwhile, the datum is shown in computer with acquisition card.

The measured points temperature are listed in Table 2. The highest temperature is 84.7 °C while the lowest temperature is 84.2 °C. Then, the error is calculated using the equation (Test temperature-Simulation temperature)*100/ Test temperature. It can be seen from the table that the maximum error is 3.07% while the minimum error is 0.7%. So the model can be used in the following simulation.

Meanwhile the grid independence is studied. The number of the grid is 50000, 60,000, 40000, respectively. When the grid number is 40000 the simulation results is not inaccurate. But when the grid number is 50000, 60,000 the simulation results are nearly the same. So the grid number is 50000 in the following simulation.

Results and Discussion

Calculated temperature fields on the surfaces of four different pipes are presented in Fig. 9. It can be found that the temperature distribution of Type (b) and Type (d) are more homogenous than Type (a) and Type (c). Therefore, Type (b) is selected as the inner structure of energy recovery system.

In order to validate the simulation results, Type (b) is manufactured, and the surface temperature is measured at the points shown in Fig. 10 using a thermocouple with an accuracy of ± 0.5 °C. The inner fluid temperature maintains at 85 °C which is similar to the simulation sets.

It is well known that the temperature in homogeneity on a solid surface can cause stress concentration, Fig. 10 shows the stress concentration induced deformation for different pipe types.

It can be seen that, comparing with Type (c), the deformation of Type (a), (b) and (d) is relatively small, and for all the four types the deformation at the central area is bigger than the other area. Although Type (c) has the most severe deformation, the maximum von-mises stress is 1.325e + 7 Pa which is still less than the material yield strength.

Table 2 Measurement results

Measure point	1	2	3	4
Test temperature(°C)	84.2	84.3	84.1	84.5
Simulation temperature(°C)	85.1	86.1	83.5	83.1
Error	− 1.06888	− 2.13523	0.713436	1.656805
Measure point	5	6	7	8
Test temperature(°C)	84.3	84.3	84.6	84.7
Simulation temperature(°C)	85.6	86	87.2	83.1
Error	− 1.54211	− 2.01661	− 3.07329	1.88902

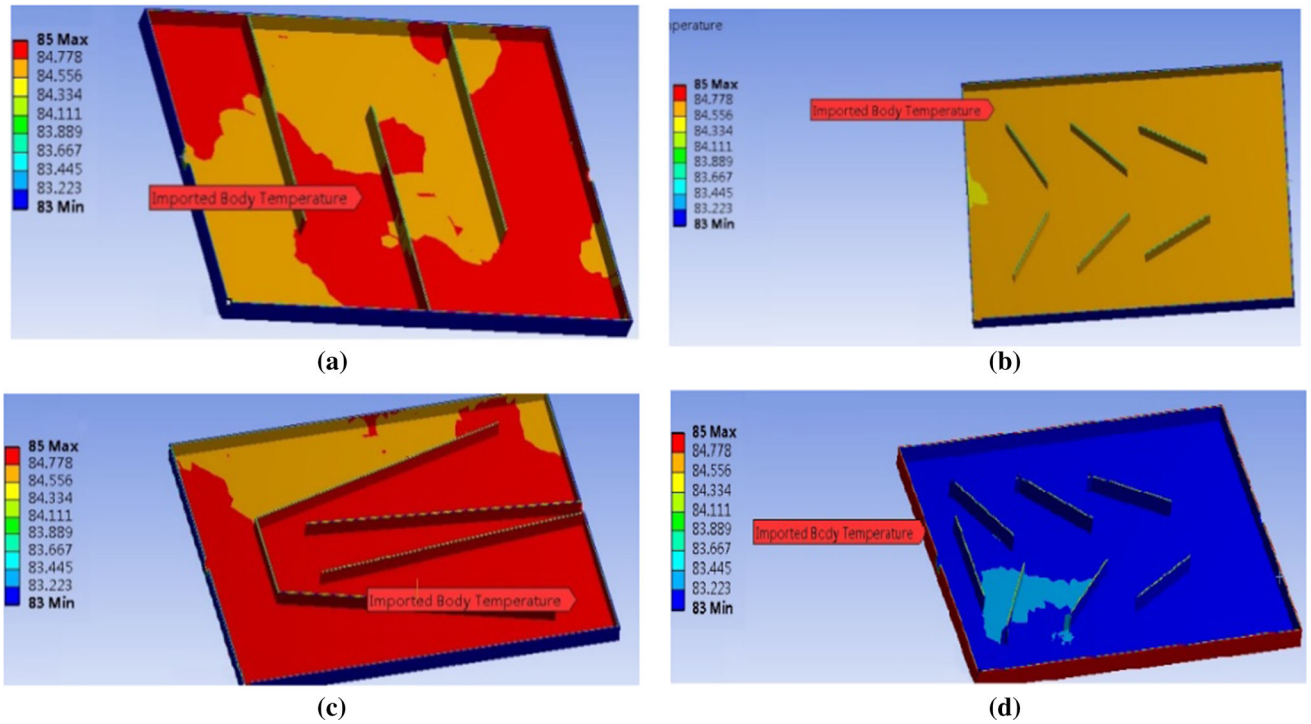

Fig. 9 Temperature field of different type structure

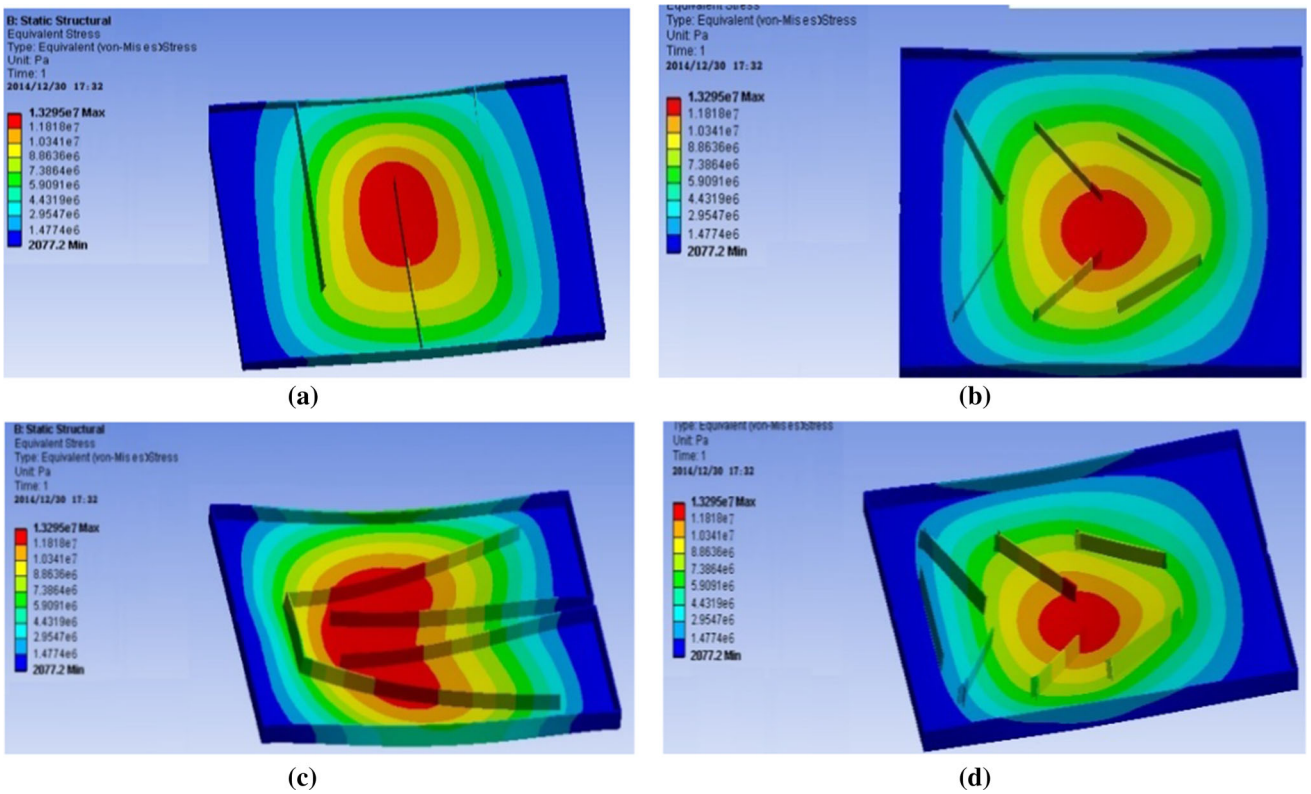

Fig. 10 Deformation of different type structure

Fig. 11 Half of the energy recovery system

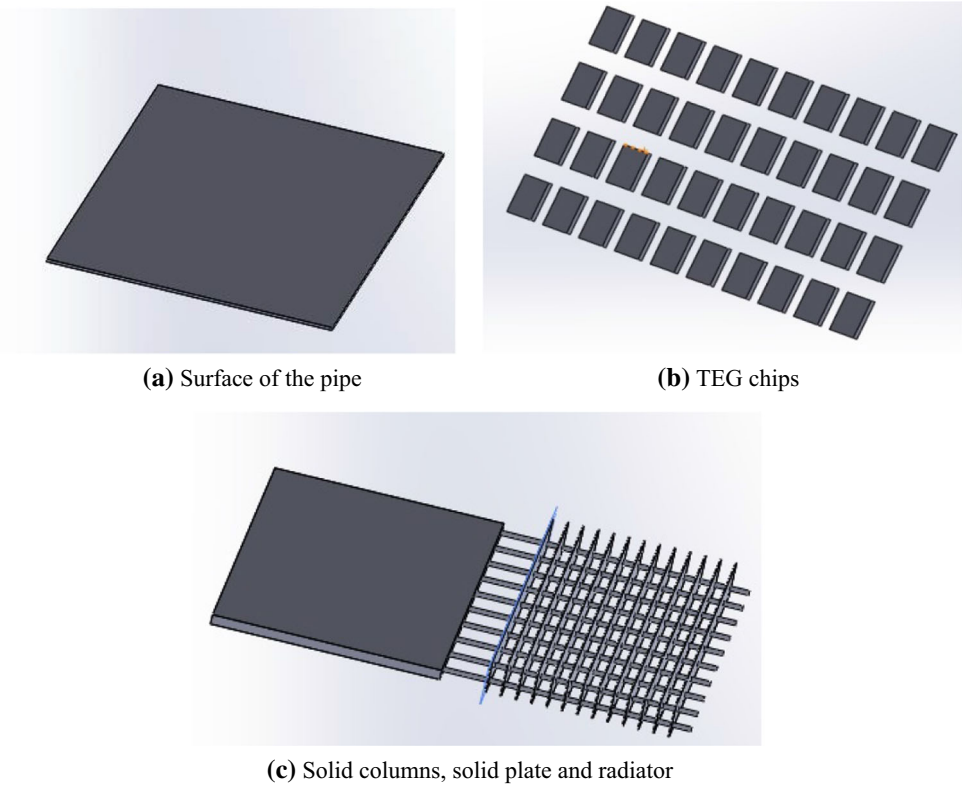

(a) Surface of the pipe

(b) TEG chips

(c) Solid columns, solid plate and radiator

Fig. 12 Mesh model

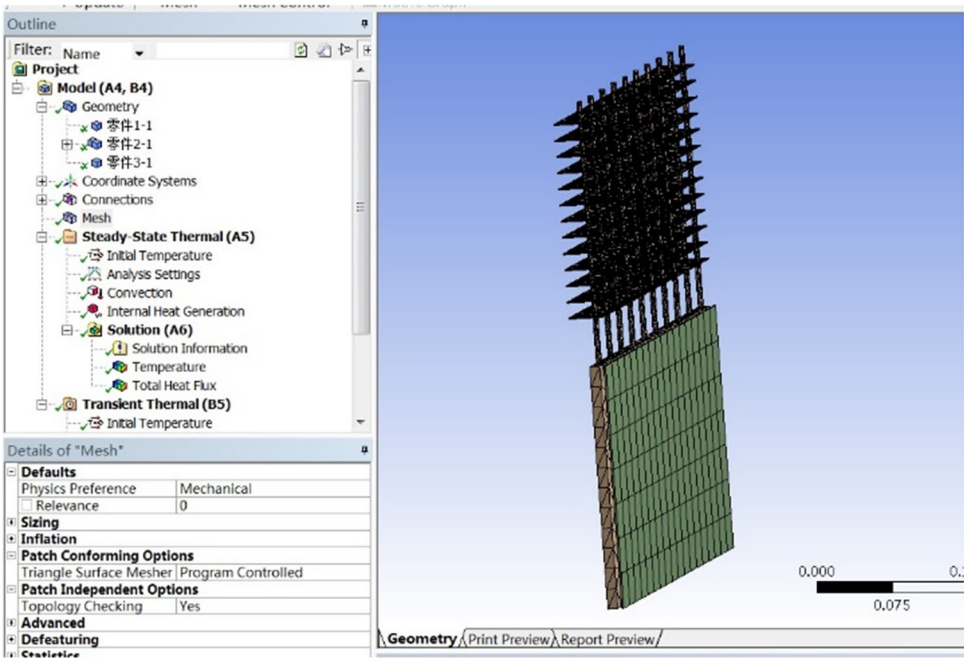

Analysis of Cooling Capacity of Cold End

For TEG system, the temperature difference has an important effect on output power and energy recovery efficient; therefore, it is very important to reduce the cold end temperature. In the application of coolant energy recovery system, the hot end temperature was almost constant because of the cooling system control strategy. So the cooling capacity of TEG can only be improved by enhancing the cold end cooling capacity. To examine the

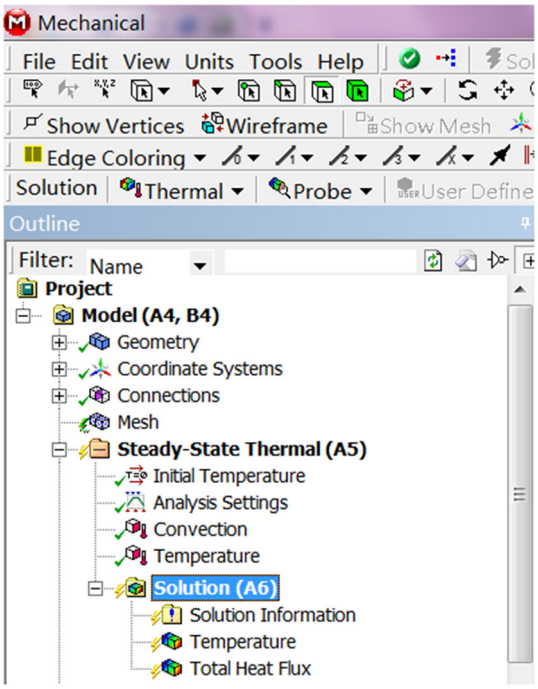

Fig. 13 Boundary condition sets

cooling capacity of cold end, an assumption should be made that the engine coolant temperature is constant. It also should be noted that the cold end includes the solid columns, solid plate and radiator.

Solid Models

Owing to the symmetrical structure of the energy recovery, a1/2 model is enough for the simulation, so only half the cold end is analyzed in this paper. The parts for the simulation are shown in Fig. 11.

Because different parts have different materials, the solid model for each part was built separately and then was assembled.

Meshing

The established solid models need to be imported into ANSYS workbench for further processing. The first step is meshing. The minimum mesh size is 1e-3 m; refined level is medium, and others parameters are set as default values. The final mesh is shown in Fig. 12.

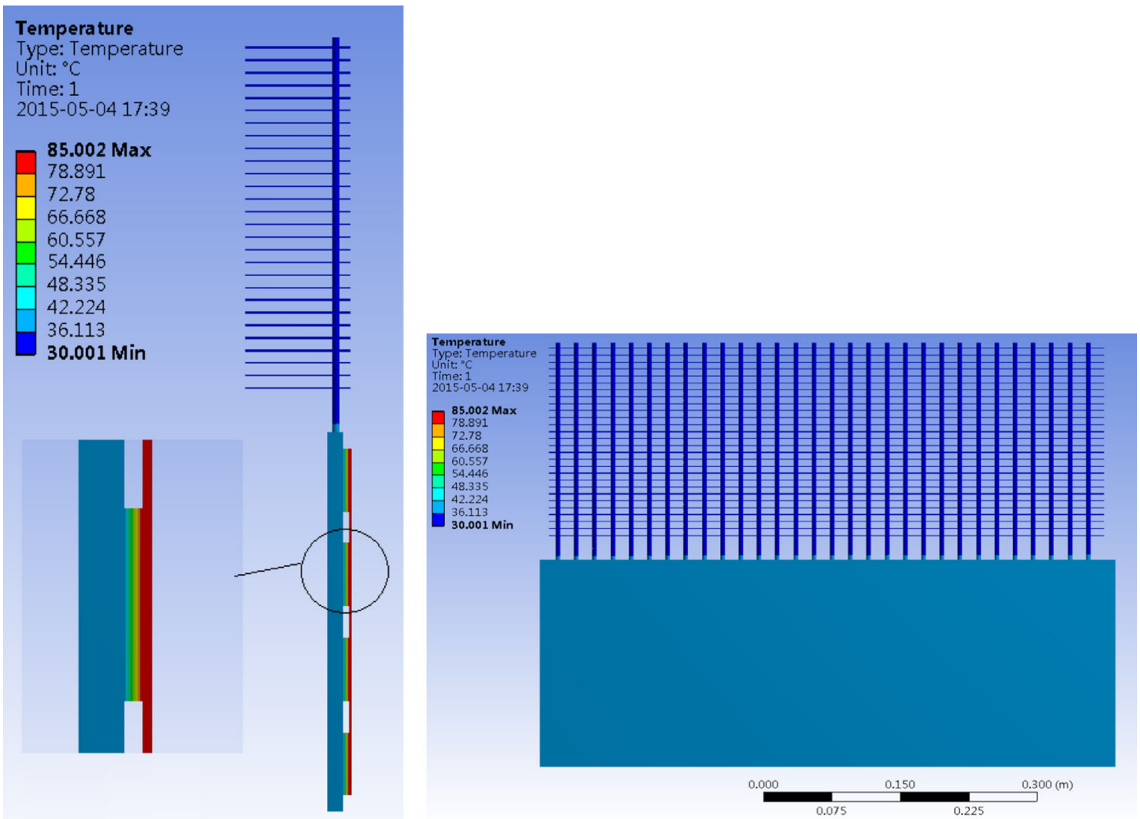

(a) Side view **(b)** Front view

Fig. 14 Temperature field of TEG without heat radiation

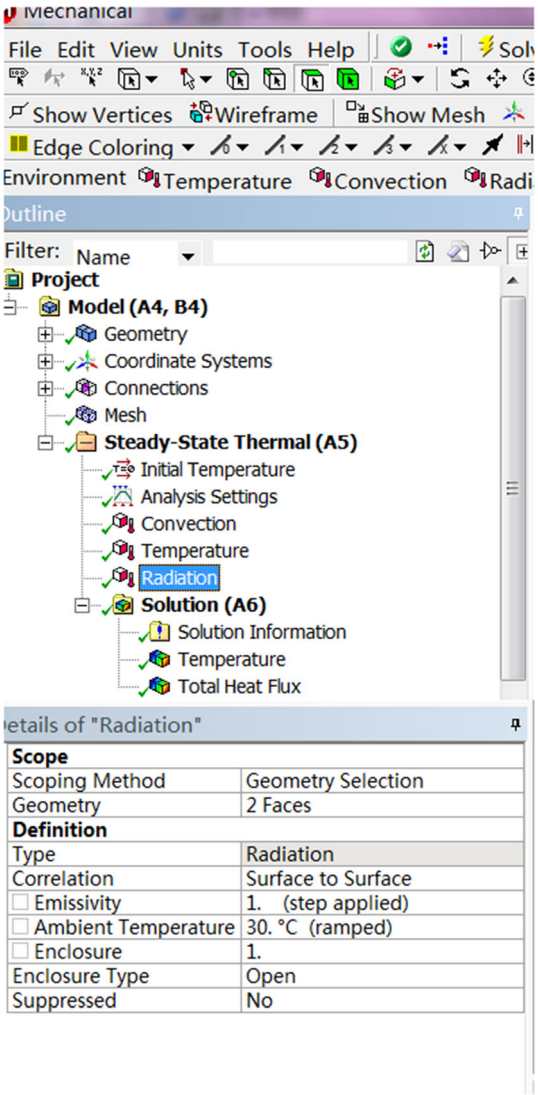

Fig. 15 Radiation constraints sets

Boundary Conditions

The material of solid columns, solid plate and radiator was aluminum alloy, and the material of TEG modules was semiconductor. The material properties were set depending on their own real properties. The thermal conductivity was set as 237 W/Mk for the aluminum alloy and 0.6 W/Mk for semiconductor.

Based on the operating condition, the coolant temperature was set as 85 °C and the surrounding temperature 30 °C. In addition, the convection should also be considered. The settings are shown in Fig. 13.

Figure 14 shows the temperature field of TEG, in which Fig. 14a is the side view and Fig. 14b the front view. It can be seen in Fig. 14a that the temperature of the pipe surface is 85 °C, which means the hot end temperature of the TEG is 85 °C. For the other parts, the temperature of contact surface between the solid plate and the TEG module is 36 °C, while the temperature of the radiator is only 30 °C, the same as the ambient temperature. However, this does not agree well with the real test.

One possibility to cause the difference between simulation and experiments may be that the above analysis does not consider the radiation effect. The distance between the TEG chip and the solid plate is only 4 mm, and the impact of radiation may not be neglected. Therefore, the following simulation is done taking into account the radiation, and the settings can be seen in Fig. 15.

The calculation results are given in Fig. 16a. It can be seen from the side view that the temperature of the contact surface between the solid plate and the TEG module has increased to 45 °C comparing with the case shown in Fig. 16b, while the inner pipe temperature is still 85 °C. Although there is still nearly 40 °C temperature difference across the TEG module, the temperature difference has been reduced comparing with Fig. 17.

The temperatures of the solid plate and the top radiator are 30 °C which is consistent with ambient temperature, and the temperature of the bottom solid plate is 45 °C. There is 15 °C difference comparing with Fig. 17. Therefore, in such a case with narrow space between TEG chip and the solid plate, radiation cannot be neglected for practical application analysis.

It also can be seen that the most of the heat is concentrated in the solid plate due to the limited heat transfer. Therefore, to increase the heat transfer, the quantity of solid column is increased from the original 30–60, and then the temperature field is re-calculated.

The calculation results are shown in Fig. 17. The temperature of the top radiator has dropped to 36 °C, and the temperature of bottom radiator is also reduced by about 5 °C.This indicates the increase of solid column quantity can effectively reduce the temperature of the cooling system and improve the cooling capacity of the cold end of TEG. However, the increase of solid column quantity will increase the cost and assembly complexity of the system.

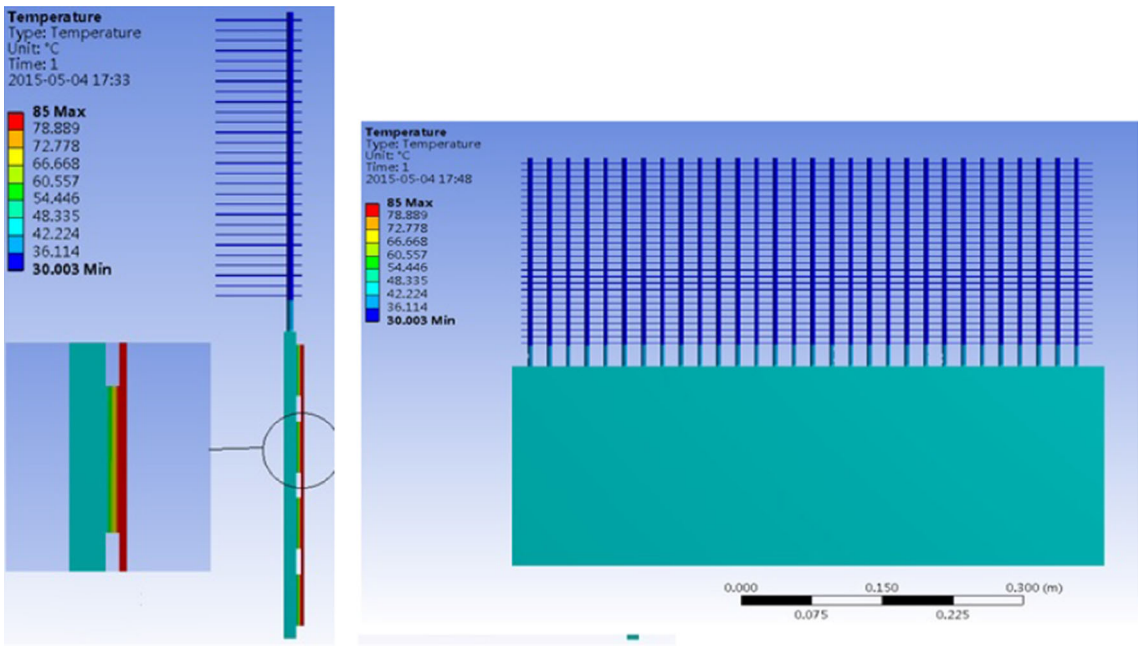

(a) Side view **(b)** Front view

Fig. 16 Temperature field of TEG with heat radiation

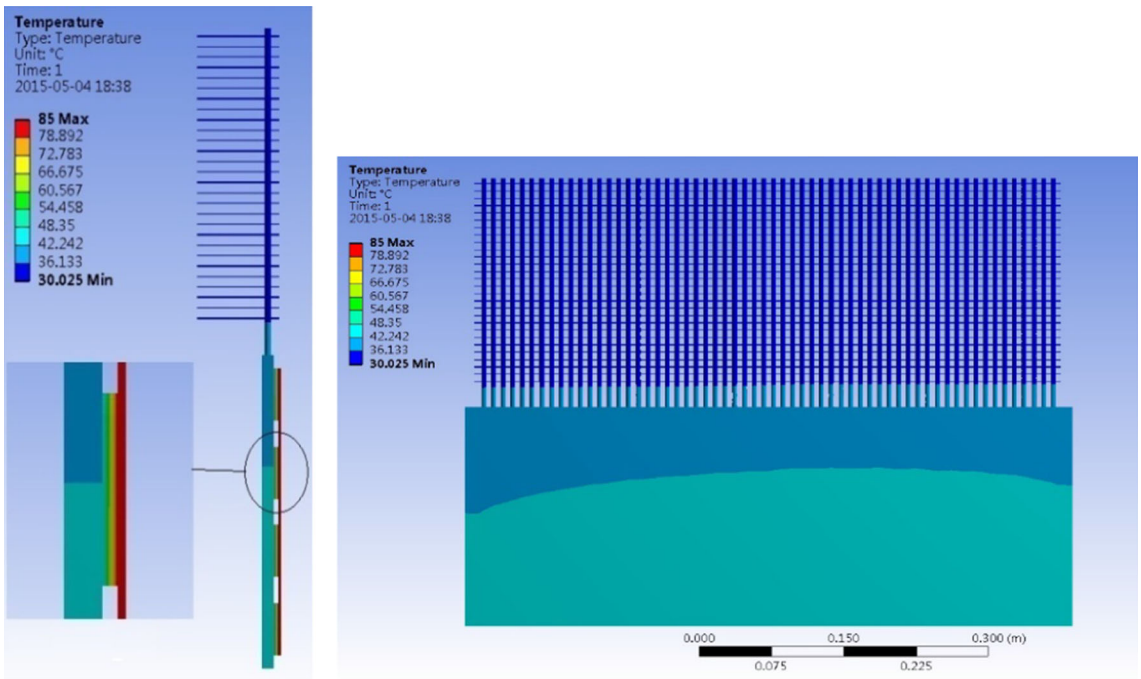

(a) Side view **(b)** Front view

Fig. 17 Temperature field of TEG when the column quantity is 60

Conclusion

In order to achieve energy recovery of the coolant heat for ICE using the TEG, the temperature field was analyzed based on ANSYS WORKBENCH software. Some conclusions can be drawn as follows.

(a) For energy recovery system, the inner structure with symmetrical baffles in the pipe is more suitable because it can achieve homogenous temperature.

(b) For the simulation of TEG system, the influence of thermal radiation needs to consider otherwise it will cause a deviation in temperature prediction.

(c) The increase of solid column quantity can effectively improve the cooling capacity of the cold end of TEG.

Acknowledgements The authors would like to express appreciation to the financial support from scientific and technological project of Henan Province (212102210332), and to Engineering Research Center of Henan Province for simulation test of coating production line.

References

1. Y. Yang, S. Wang, W. He, Simulation study on regenerative thermoelectric generators for dynamic waste heat recovery. Energy Procedia. **158**, 571–576 (2019)
2. S. Lan, A. Smith, R. Stobart et al., Feasibility study on a vehicular thermoelectric generator for both waste heat recovery and engine oil warm-up. Appl. Energy **242**, 273–284 (2019)
3. Y.A. Chaboki, A. Khoshgard, G. Salehi et al., Energy, exergy, and environmental analysis of meeting cooling demand of a ship with waste heat recovery. Energ. Effi. **14**(2), 1–14 (2021)
4. R. Prakash, D. Christopher, K. Kumarrathinam, Analysis of Surface Waste Heat Recovery in IC Engine by Using TEG. Appl. Mech. Mater. **787**, 782–786 (2015)
5. C. Daniel, Thermoelectric generators: A review of applications. Energy Conver. Manage. **140**, 167–181 (2017)
6. Q. Wan, Y.K. Teh, Y. Gao, P. Mok, Analysis and design of a thermoelectric energy harvesting system with reconfigurable array of thermoelectric generators for IoT applications. IEEE Trans. Circuits Syst. I Regular Papers. **99**, 1–13 (2017)
7. M. Kohl, M. Gueltig, F. Wendler, Coupled simulation of thermo magnetic energy generation based on NiMnGaHeusler alloy films. Shape Memory Super Elasticity. **4**, 1–14 (2018)
8. C. Liu, Z.L. Wei, An experimental study of a novel prototype for thermoelectric power generation from vehicle exhaust. Cogener. Competitive Power J. **28**, 32–48 (2014)
9. Z.Z. Ma, X.P. Yan, H.S. Ma et al., Effects of temperature on characters of the thermoelectric generator using in lng energy recovery. Int. J. Electr. Eng. **26**(6), 237–244 (2019)
10. Z.Z. Ma, H.M. Zhang, A.J. Yang, Designs of exhaust gas thermoelectric generator and experiment test. Machinery Design Manuf. **311**, 130–133 (2017)
11. Z.Z. Ma, P. Xu, X.L. Wang, Design and development of simulation test platform for thermoelectric generation of engine cooling system. Experim. Technol. Manag. **34**, 90–94 (2017)
12. C.Y. Wang, Y.Z. Li, J. Zheng, Study on thermoelectric power generator with large temperature difference between LNG and exhaust gas. Chinese Journal of Power Sources **40**, 149–152 (2016)
13. C.S. Kim, G. Lee, S, Choi H. Structural design of a flexible thermoelectric power generator for wearable applications. Appl. Energy. **214**, 131–138 (2018)
14. P. Yu, X.W. Sun, Y. Zeng, The numerical analysis on the heat transfer performance of CPU heat sink cooled by vertical uniform jet. J. Eng. Thermo Phys. **24**, 415–418 (2003)
15. X. Niu, J.L. Yu, S.Z. Wang, Experimental study on low-temperature waste heat thermoelectric generator. J. Power Sour. **188**, 621–626 (2009)
16. A.K. Nikolay, S.K. Viktor, A.P. Igor, Thermoelectric cooling system for internal combustion engine. Part1: development of the technical aspects. Int. J. Appl. Eng. Res. **11**, 847–855 (2016)